Analysis of the Drying Rate during the Falling Rate Period in the Drying of a Bed of Granular and Powdered Materials

AUTHOR(S):

TOEI, Ryozo; HAYASHI, Shinya

CITATION:

TOEI, Ryozo ...[et al]. Analysis of the Drying Rate during the Falling Rate Period in the Drying of a Bed of Granular and Powdered Materials. Memoirs of the Faculty of Engineering, Kyoto University 1965, 27(3): 303-316

ISSUE DATE:

1965-08-31

URL:

http://hdl.handle.net/2433/280632

Analysis of the Drying Rate during the Falling Rate Period in the Drying of a Bed of Granular and Powdered Materials

By

Ryozo TOEI* and Shinya HAYASHI*

(Received March 31, 1965)

Drying mechanism of a bed of granular and powdered materials during the first falling rate period was analysed.

The drying rate curves obtained from the present analysis represent sufficiently the experimental drying rate curves.

Drying mechanism during the second falling rate period was analysed from the same considerations.

The drying mechanism must be analysed as the phenomena of a simultaneous heat and mass transfer. Drying periods of a bed of non-adsorptive granular and powdered materials are distinguished to constant rate period, first and second falling rate periods from experimental results. The drying mechanism during the second falling rate period was analysed from such consideration in our previous reports.[1,2]

In this report, we will discuss the mechanism for the first falling rate period. The same argument is applied to the second falling rate period also.

1. Drying Mechanism of the First Falling Rate Period

From our experimental results, the moisture distribution in the drying process can be shown generally as described in **Fig. 1.** The critical moisture content, at which the constant rate period finishes and the first falling rate period begins, is represented by w_c in this figure. The second critical moisture content, at which the second falling rate period begins, is represented by w_p. The surface moisture content becomes the equilibrium moisture content, at the second critical moisture content. The first falling rate period is situated at the intermediate moisture content between w_c and w_p. It is usually considered that the constant rate of drying corresponds to the surface evaporation rate and the moisture is transported to the surface by the liquid

* Department of Chemical Engineering

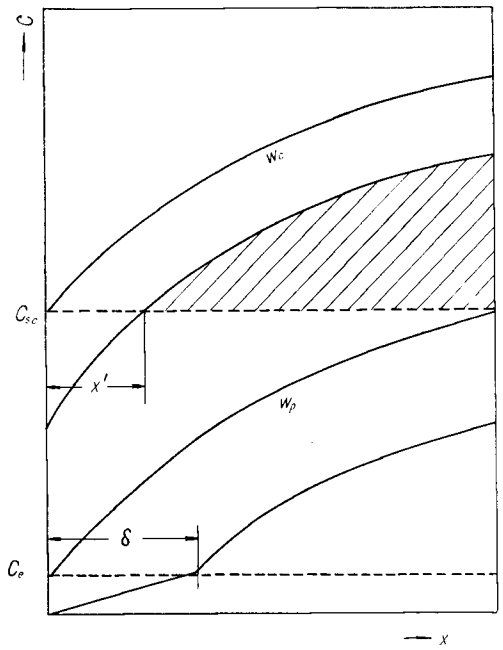

Fig. 1. Schematic moisture distribution curves in the bed during the drying process

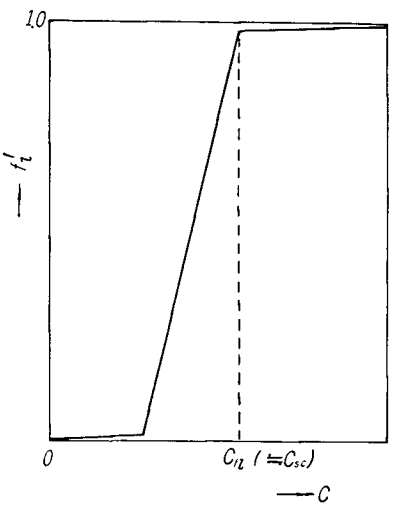

Fig. 2. Schematic representation of the relation of the local liquid fraction of moisture transfer f_l' vs. the moisture content c

form during the period. The moisture transfer rate decreases below the critical moisture content and is less than the surface evaporation rate. So the evaporation occurs at the interior of the bed. To evaluate the degree of the internal evaporation, the drying experiment of the bed containing NaCl solution was performed.[3] In such experiment the movement of salt is caused mostly by only the liquid moisture transfer. The liquid fraction of moisture transfer is defined and these numerical values were calculated from the data of the moisture distribution and salt distribution. The liquid fraction of moisture transfer is affected mainly by moisture content and is not affected by the external drying conditions. **Fig. 2** shows the schematical relation of the local liquid fraction of moisture transfer f_l' vs. the moisture content c. It was recognized that the value of f_l' is equal to 1, i. e. only the liquid moisture transfer occurs during the constant rate period. The moisture content at which f_l' begins to decrease from 1 is nearly equal to the surface moisture content at w_c. Below the critical moisture content the surface moisture content decreases from c_{sc} and the plane holding the moisture content c_{sc} retreats into the bed. The internal evaporation occurs considerably in the region of $0 \sim x'$ in which the moisture content has become below c_{sc}. On the

otherhand, the internal evaporation does not occur and the liquid moisture transfer predominates in the region of $x' \sim L$ in which the moisture content remains above c_{sc}. The later transfer mechanism is the same situation as in the constant rate period and could not be a rate controlling step duriug the first falling rate period. It can be considered that the rate controlling steps during the first falling rate period are the mass transfer resistance at surface air film and in the region of $0 \sim x'$. The moisture is transported by vapor transfer in this region. So the simultaneous heat and mass transfer must be considered in the region of $0 \sim x'$. The system of these differential equations describing the process of heat and mass transfer in the drying bed is very difficult for finding the adequate solution. Although A. V. Luikov and Y. Mikhailov[4] have done a great deal of work on the analytical solution of this system, their argument is restricted to the case of the constant transfer coefficients. In the practical case, the all transfer coefficients are variable parameters. Furthermore the distance x' moves with time, so we must treat the moving boundary problem. It is scarcely possible to analyze such a problem. To simplify the system of transfer equations, we adopt a kind of "pseudo steady state approximation". That is to say that the state of vapor transfer becomes steady state at any liquid moisture distributions. Accordingly the moving boundary problem of the vaper transfer can be relieved of the consideration. The state of liquid moisture distribution is evaluated from our experimental results so that the moisture distribution curves shift retaining their parabolic forms.

2. Analysis of the Drying Rate during the First Falling Rate Period

In this report the drying mechanism is analysed as a mass transfer pro-

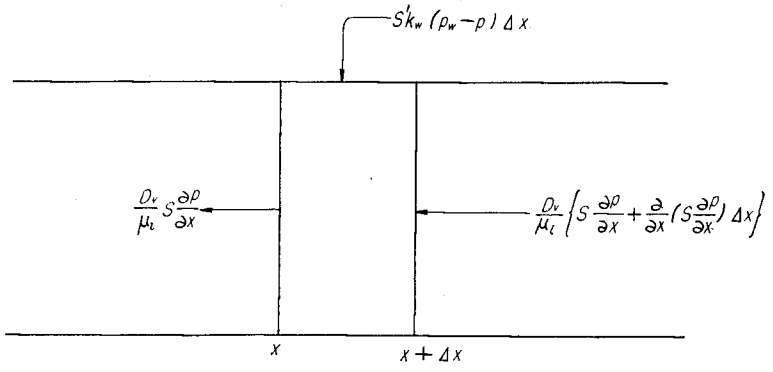

Fig. 3. Element of thin shell at which a mass balance is made

blem. As mentioned in the previous section, we may consider the vapor transfer at any moisture distributions. A mass balance is made over a thin shell bounded by the planes x and $x+\Delta x$ as shown in **Fig. 3.** Considering that the vapor diffusion is caused by the pressure gradient, the following vapor transfar equation can be obtained;

$$s\frac{\partial p}{\partial \theta} = \frac{D_v}{\mu_1}\frac{\partial}{\partial x}\left(s\frac{\partial p}{\partial x}\right)+s'k_w(p_w-p) \tag{1}$$

The last term of right hand side of Eq. (1) represents the internal evaporation rate. The symbol s represents the effective pore area per unit area and is considered to be given by Eq. (2);

$$s = \varepsilon' = \varepsilon-\varphi = \varepsilon-\frac{\rho'}{\rho_w}c = \varepsilon-\alpha c \tag{2}$$

Where c is given by a parabolic form;

$$c = c_m-(c_{mc}-c_{sc})\left(1-\frac{x}{L}\right)^2 \tag{3}$$

According to Eq. (2), s varies with moisture content but slightly, so s may be replaced by the value of average moisture content $\bar{c}$.

$$s = \varepsilon-\alpha\bar{c} \tag{2'}$$

The symbol s' represents the wetted length per unit area. About the dried bed it can be given as length of circumference of cross section of particles.

$$s'_{\mathrm{dry}} = \frac{\sum n_i\pi d_{pi}}{\sum n_i\pi d_{pi}^2/4(1-\varepsilon)} = \frac{4}{\bar{d}_p}(1-\varepsilon) \tag{4}$$

Then the wetted length at moisture content c may be assumed by the following Eq. (5),

$$s' = s'_{\mathrm{dry}}\left(\frac{c}{c_{sc}}\right) = \frac{4}{\bar{d}_p}(1-\varepsilon)\left(\frac{c}{c_{sc}}\right) \tag{5}$$

The constant μ_1, resistance coefficient for vapor diffusion, is given by Krischer[5] as 1.57 in the case of a random packing of dried spherical particles. But usually this value is taken as $\mu_1=1$, so our calculation is performed as $\mu_1=1$.

The vapor transfer equation becomes to;

$$(\varepsilon-\alpha\bar{c})\frac{\partial p}{\partial \theta} = (\varepsilon-\alpha\bar{c})D_v\frac{\partial^2 p}{\partial x^2}+4\left(\frac{c}{c_{sc}}\right)\frac{(1-\varepsilon)}{\bar{d}_p}k_w(p_w-p) \tag{6}$$

Assuming the steady state, i.e. $\frac{\partial p}{\partial \theta}=0$

$$(\varepsilon-\alpha\bar{c})D_v\frac{\partial^2 p}{\partial x^2}+4\left(\frac{c}{c_{sc}}\right)\frac{(1-\varepsilon)}{\bar{d}_p}k_w(p_w-p)=0 \tag{7}$$

Boundary conditions are as follows.

The boundary condition at surface is considered as follows;

$$D_v\varepsilon_0'\frac{\partial p}{\partial x}+\text{surface evaporation rate}=k_g(p-p_a) \qquad \text{at } x=0 \tag{8}$$

The value of the surface evaporation rate may be estimated as follows;

$$\text{surface evaporation rate}=\left(\frac{c_s}{c_{sc}}\right)^m k_g(p_{x=0}-p_a) \tag{9}$$

From Eqs. (8) and (9),

$$D_v\varepsilon_0'\frac{\partial p}{\partial x}=k_g\left\{1-\left(\frac{c_s}{c_{sc}}\right)^m\right\}(p-p_a)=k_g'(p-p_a) \qquad \text{at } x=0 \tag{10}$$

where

$$k_g'=k_g\left\{1-\left(\frac{c_s}{c_{sc}}\right)^m\right\} \tag{11}$$

Another boundary condition is as follows;

$$p=p_w \qquad \text{at } x=x' \tag{12}$$

The later condition is deduced from the consideration that the plane at $x=x'$ is the deepest internal evaporation plane. Rewriting the variables by $X=1-\frac{x}{L}$ and $p_w-p=p'$, Eq. (7) becomes;

$$\frac{\partial^2 p'}{\partial X^2}-K\left(\frac{A-DX^2}{a}\right)p'=0 \tag{13}$$

where

$$a=\frac{D_v(\varepsilon-\alpha\bar{c})}{L^2}, \qquad A=c_m$$
$$D=(c_{mc}-c_{sc}), \qquad K=\frac{4(1-\varepsilon)k_w}{\bar{d}_p c_{sc}} \tag{14}$$

Boundary conditions become;

$$D_v\varepsilon_0'\frac{\partial p'}{\partial X}=k_g'(p_w-p_a-p') \qquad \text{at } X=1 \tag{15}$$

$$p'=0 \qquad \text{at } X=X'=\left(1-\frac{x'}{L}\right) \tag{16}$$

Eq. (10) can be solved by W. K. B. method. The solution is as follows;

$$p'=p_w-p=\mathfrak{A}_1\exp\{\sqrt{K}\,\varphi(X)\}+\mathfrak{B}_1\exp\{-\sqrt{K}\,\varphi(X)\} \tag{17}$$

The constants $\mathfrak{A}_1$ and $\mathfrak{B}_1$ are determined by the boundary conditions;

$$\mathfrak{A}_1 = \frac{-k_g'(p_w-p_a)\exp\{-\sqrt{K}\,\varphi(X')\}}{(-M+k_g')\exp\{-\sqrt{K}\,f(X')\}-(M+k_g')\exp\{\sqrt{K}\,f(X')\}} \tag{18}$$

$$\mathfrak{B}_1 = \frac{k_g'(p_w-p_a)\exp\{\sqrt{K}\,\varphi(X')\}}{(-M+k_g')\exp\{-\sqrt{K}\,f(X')\}-(M+k_g')\exp\{\sqrt{K}\,f(X')\}} \tag{19}$$

where

$$\varphi(X) = \int_0^X \sqrt{\frac{A-DX^2}{a}}\,dX = \sqrt{\frac{D}{a}}\left[\frac{X}{2}\sqrt{\frac{A}{D}-X^2}+\frac{A}{2D}\sin^{-1}\sqrt{\frac{D}{A}}\,X\right] \tag{20}$$

$$f(X) = \varphi(1)-\varphi(X) \tag{21}$$

$$M = \frac{D_v\varepsilon_0'}{L}\sqrt{K}\sqrt{\frac{A-D}{a}} \tag{22}$$

The expression for the drying rate R can be obtained from Eq. (23);

$$\begin{aligned} \mathrm{R} &= \rho' L\frac{-dw}{d\theta} = \frac{k_g}{R_w T_{av}}(p_{X=1}-p_a) \\ &= \frac{k_g}{R_w T_{av}}(p_w-p_a)\left\{1-\frac{k_g'}{M\coth\{Kf(X')\}+k_g'}\right\} \end{aligned} \tag{23}$$

In order to connect R by Eq. (23) with average moistuse content w, the relation between X' and w must be found. Considering that the change of moisture distribution is the parallel shifting of parabolas, the following ralation between X' and w can be obtained by geometrical calculation;

$$X' = \sqrt{1-\frac{2(w_c-w)}{3(w_p-c_e)}} \tag{24}$$

The values of the constants which are included in A, D and a of Eq. (14) can be obtained from the experimental results or literature. The mass transfer coefficient, k_g, are obtained from data of the constant drying rate as follows;

$$k_g = \frac{R_w T\rho' L}{(p_w-p_a)}\left(\frac{-dw}{d\theta}\right)_{\text{const}} \tag{25}$$

The coefficient of water vapor diffusion in air, D_v, can be obtained from the literature.[6]

The value k_g' is calculated by Eq. (12), where m is taken as one.

The values of p_w in Eq. (23) are taken as the saturated vapor pressure at the respective material temperature, which is determined by the experimental data. The drying rate curves are calculated in the case of drying of the sand bed by the above consideration. The calculated results are shown in **Fig. 4, 5, 6 and 7** comparing with the experimental ones. Good agreements can be obtained.

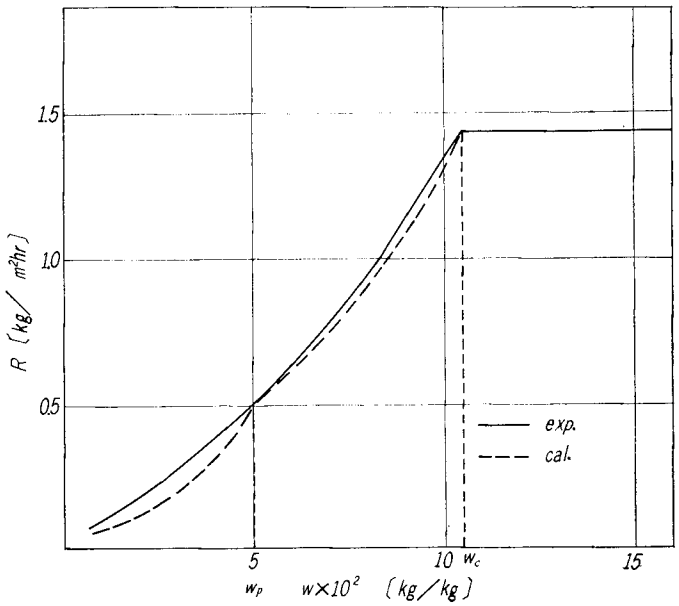

Fig. 4. Comparison between experimental and calculated drying rate curve (Run No s-3-50, sand (28～35#), t_a=50°C, H_a=0.0076 V_a=5.48 m/sec, L=0.03 m)

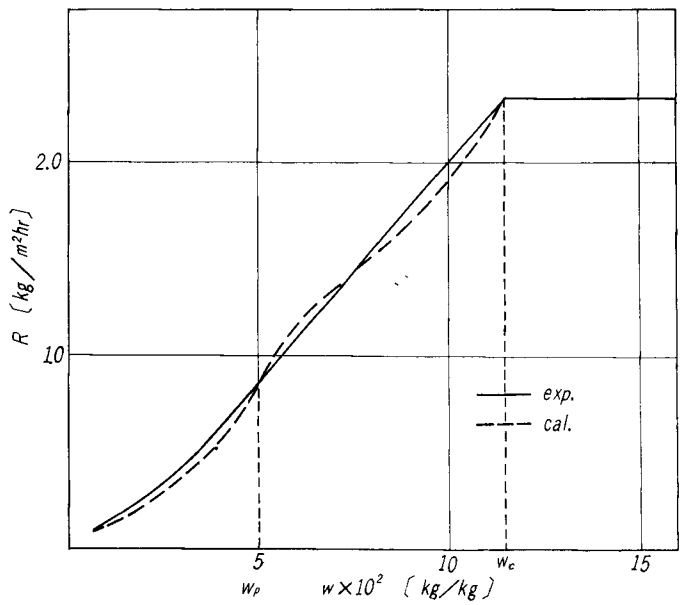

Fig. 5. Comparison between experimental and calculated drying rate curve (Run No s-3-70, sand (60～80#), t_a=70°C, H_a=0.0076, V_a=5.15 m/sec, L=0.03 m)

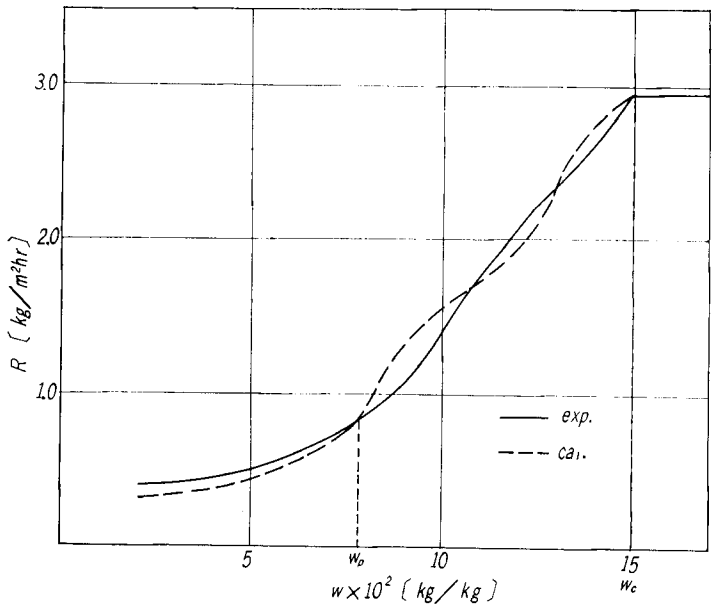

Fig. 6. Comparison between experimental and calculated drying rate curve (Run No s-5-70, sand (28~35#), t_a=70°C, H_a=0.0076, V_a=5.77 m/sec, L=0.05 m)

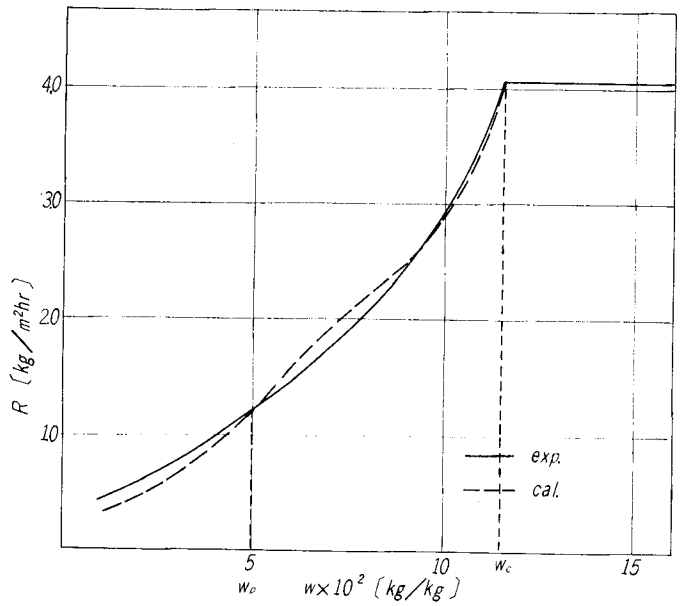

Fig. 7. Comparison between experimental and calculated drying rate curve (Run No s-3-95, sand (28~35#), t_a=95°C, H_a=0.0076, V_a=5.63 m/sec, L=0.03 m)

Table 1 shows the values of k_w, which are used in these examples. The values of k_w ranged between 1 and 9 are independent on temperature and diameter of particles.

Table 1.

Run No	s-3-50	s-3-70	s-3-70	s-22	s-3-95	s-5-70
t_a (°C)	50	70	70	70.3	95	70
$\bar{d}_p$ (μ)	503	210.5	503	210.5	503	503
k_w	5.76	2.9	1.85	1	7.3	9

In the case of calcium carbonate the actual particle diameter is 1μ, but the particles are aggregated. So the effective particle diameter is estimated as 30μ. The example of the calculated drying rate curve is shown in **Fig. 8** with the experimental drying rate curve. The value of k_w is taken one in this case.

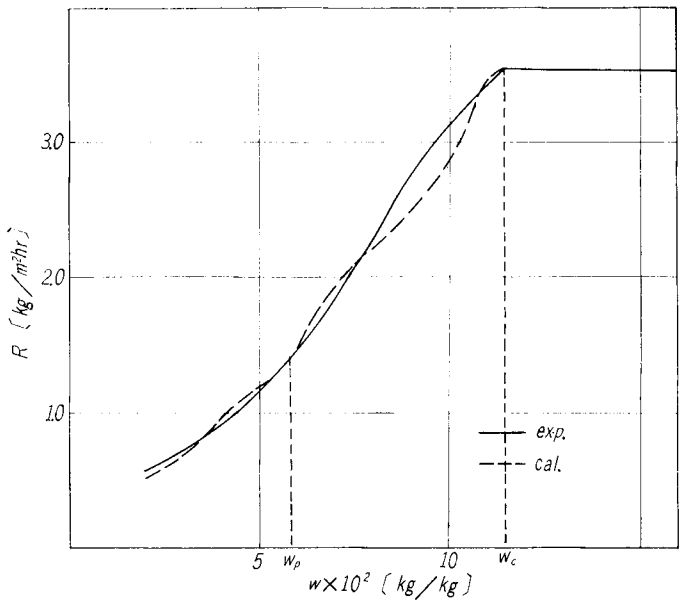

Fig. 8. Comparison between experimental and calculated drying rate curve (Run No 3-90, $CaCO_3$, t_a=90°C, H_a=0.0076, V_a=5.58 m/sec, L=0.03 m)

It is considered the drying mechanism proposed in this report is correct from the agreement between the calculated drying rate curves and the experimental ones. The analysis according to the simultaneous heat and mass transfer will be needed to express more exactly the mechanism of the drying process.

3. Analysis of the Drying Rate during the Second Falling Rate Period

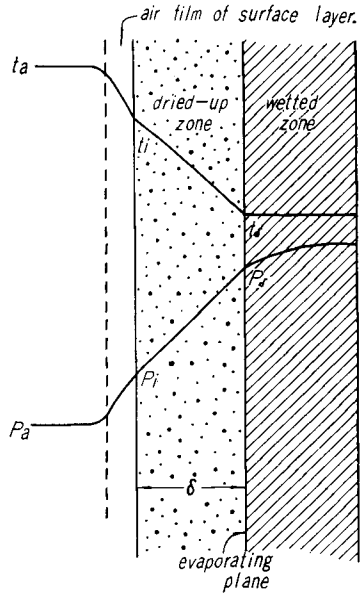

Fig. 9. Schematic model of evaporation surface of bed in the second falling rate period

Fig. 9 shows the schematic model of the drying mechanism during the second falling rate period proposed in our previous report.[1] The bed is separated into two zones, i. e. the dried-up zone and the weeted zone, and the drying proceeds by the vapor transfer through the dried-up zone. Considering the balance of heat and mass transfer on the dried-up zone, the following relation is established;

$$\frac{(t_a-t_\delta)}{\left(\frac{1}{h_p}+\frac{\delta}{\lambda}\right)r_\delta} = \frac{1}{\left(\frac{1}{k_g}+\frac{\delta}{\varepsilon D_v}\right)}\left(\frac{p_\delta}{R_w T_\delta}-\frac{p_a}{R_w T_a}\right) \tag{26}$$

In our previous report,[1] p_δ was assumed to be the saturated vapor pressure corresponding to the value of t_δ, and then the asymptotic temperature t_p was analysed at the condition $1/h_p \ll \delta/\lambda$, $1/k_g \ll \delta/\varepsilon D_v$ $(\delta \to \infty)$.

According to the consideration in this report, more rigorous treatment of p_δ and t_δ is possible. The mass transfer problem in the wetted zone is considered in the same manner as previous chapter.

$$\left(\varepsilon-\frac{\rho}{\rho_s}\bar{c}\right)D_v\frac{\partial^2 p}{\partial x^2}+\frac{4(1-\varepsilon)}{d_p}\left(\frac{c}{c_{sc}}\right)k_w(p_w-p)=0 \tag{27}$$

For the example, at the sand bed, the moisture distribution is represented by the paralell shifting of parabolas from experimental results.

So the moisture distribution is represented by Eq. (28);

$$c=(c_{mc}-c_{sc})\left\{\left(1-\frac{\delta}{L}\right)^2-\left(1-\frac{x}{L}\right)^2\right\}+c_e \tag{28}$$

Eq. (29) can be derived from Eq. (28).

$$\left(1-\frac{\delta}{L}\right)=\left(\frac{w-c_e}{w_p-c_e}\right)^{1/3} \tag{29}$$

The boundary conditions for Eq. (28) are as follows,

$$\left(1-\frac{c_e}{c_{sc}}\right)\frac{(p-p_a)}{\dfrac{1}{k_g}+\dfrac{\delta}{\varepsilon D_v}}=\varepsilon D_v\frac{\partial p}{\partial x} \qquad \text{at} \quad x=\delta \tag{28}'$$

$$p=p_w, \qquad \text{at } x=L \text{ (if the region, } c>c_{sc}\text{, exits, } x=x') \tag{29}'$$

The later condition is based on the consideration that the vapor pressure at the bottom is almost nearly equal to the equilibrium vapor pressure as the resistance for vapor transfer through the bed is so much. From our other experiments, the equilibrium vapor pressure of the wetted material (for example, sand) is equal to the saturated vapor pressure except the extreme low moisture content.

The solution of Eqs. (27), (28) and (29) is deduced by the W. K. B. method.

$$p_w-p=\mathfrak{A}_2\exp\{\sqrt{K}\,\varphi(X)\}+\mathfrak{B}_2\exp\{-\sqrt{K}\,\varphi(X)\} \tag{30}$$

where

$$\left.\begin{aligned} K&=\frac{4(1-\varepsilon)}{d_p c_{sc}}k_w, \qquad \varphi(X)=L\sqrt{\frac{1}{\varepsilon D_v}}\int_D^X c(X)\,dx \\ X&=1-\frac{x}{L}, \qquad \Delta=1-\frac{\delta}{L} \end{aligned}\right\} \tag{31}$$

$$\left.\begin{aligned} \mathfrak{A}_2&=\frac{-\alpha'(p_w-p_a)\exp\{-\sqrt{K}+\varphi(X')\}}{(-N+\alpha')\exp\{-\sqrt{K}\,(\varphi(\Delta)-\varphi(X))\}-(N+\alpha')\exp\{\sqrt{K}(\varphi(\Delta)-\varphi(X))\}} \\ \mathfrak{B}_2&=\frac{\alpha'(p_w-p_a)\exp\{\sqrt{K}\,\varphi(X')\}}{(-N+\alpha')\exp\{-\sqrt{K}\,(\varphi(\Delta)-\varphi(X))\}-(N+\alpha')\exp\{\sqrt{K}(\varphi(\Delta)-\varphi(X))\}} \end{aligned}\right\} \tag{32}$$

$$\left.\begin{aligned} N&=\sqrt{\varepsilon D_v K c_e} \\ \alpha'&=\left(1-\frac{c_e}{c_{sc}}\right)\left(\frac{1}{\dfrac{1}{k_g}+\dfrac{\delta}{\varepsilon D_v}}\right) \end{aligned}\right\} \tag{33}$$

The value of p_δ can be calculated by Eqs. (30)~(33), because the temperature in the wetted zone is almost uniform. Inserting the relation of p_δ from Eqs. (30)~(33) in Eq. (26),

$$\begin{aligned} &r_\delta\left(\frac{1}{h_p}+\frac{\delta}{\lambda}\right)\left(\frac{1}{\dfrac{1}{k_g}+\dfrac{\delta}{\varepsilon D_v}}\right)\left(1-\frac{\alpha'}{N\coth\sqrt{K}f(\Delta)+\alpha'}\right) \\ &\quad=\frac{(t_a-t_\delta)}{\dfrac{p_w}{R_w T_\delta}-\dfrac{p_a}{R_w T_a}} \end{aligned} \tag{34}$$

The value of t_δ, temperature of the boundary plane between two zones, can be calculated by Eq. (34).

Table 2 shows the examples of the calculated results with experimental

values. The good agreement is observed. The drying rate during the second falling rate period can be deduced from Eq. (34).

Table 2.

Run No s-3-50 (28~35#)

w	0.05	0.04	0.03	0.04	0.05
t_δ cal °C	38.6	38.9	39.1	39.2	39.8
t_δ exp °C	38.3	39.0	39.3	39.3	39.8

Run No s-3-70 (60~80#)

w	0.05	0.04	0.03	0.02	0.01
t_δ cal °C	50.7	51.6	51.6	51.8	52.5
t_δ exp °C	50.9	52.0	52.7	52.9	52.4

Run No s-5-70 (28~35#)

w	0.08	0.07	0.06	0.05	0.04	0.03	0.02
t_δ cal °C	50.6	50.6	51.0	51.0	51.0	51.0	51.2
t_δ exp °C	48.0	50.0	50.0	50.0	50.5	52.0	53.2

Run No s-3-95 (28~35#)

w	0.05	0.04	0.03	0.02
t_δ cal °C	59.8	60.0	60.0	60.6
t_δ exp °C	59.7	60.4	60.4	60.4

Run No 3-90 ($CaCO_3$)

w	0.05	0.04	0.03	0.02	0.01
t_δ cal °C	57.9	58.5	62.1	64.3	65.4
t_δ exp °C	53.2	58.3	60.4	62.0	63.1

$$\mathrm{R} = -\rho' L\left(\frac{dw}{d\theta}\right) = \frac{1}{\frac{1}{k_g}+\frac{\delta}{\varepsilon D_v}}\left(\frac{p_\delta}{R_w T_\delta}-\frac{p_a}{R_w T_a}\right)$$

$$\fallingdotseq \frac{1}{R_w T_{av}}\left(\frac{1}{\frac{1}{k_g}+\frac{\delta}{\varepsilon D_v}}\right)(p_\delta - p_a)$$

$$= \frac{1}{R_w T_{av}}\left(\frac{1}{\frac{1}{k_g}+\frac{\delta}{\varepsilon D_v}}\right)(p_w - p_a)\left(1-\frac{\alpha'}{N\coth\{\sqrt{K f(\Delta)}\}+\alpha'}\right) \tag{35}$$

where

$$f(\Delta) = \varphi(\Delta) - \varphi(X) \tag{36}$$

The calculated drying rate curves using the calculated value of t_δ in Table 2 are shown in Fig. 4~8. Good agreements are observed between the calculated results and experimental ones.

4. Conclusion

Drying mechanism of a bed of non-adsorptive granular and powdered materials during the first falling rate period was analysed. From our previous experimental results the rate controlling steps during the first falling rate period may be considered as the mass transfer resistance at surface air film and in the region of bed at which the internal evaporation occurs. The problem of the vapor transfer in this period was analysed, using a kind of pseudo steady state approximation method. The drying rate curves calculated from the present analysis represent sufficiently the experimental drying rate curves. The mechanism of the second falling rate period was also analysed from the same analysis and the drying rate curve and the behaviors of the temperature of the boundary plane between the dried-up zone and the wetted zone are calculated.

Literature Cited

1) R. Toei and S. Hayashi: The Memoirs of the Faculty of Engng., Kyoto University **25** 457 (1963).
2) R. Toei and S. Hayashi: ibid **26** 208 (1964).
3) R. Toei and S. Hayashi: ibid **27** 218 (1965).
4) A. V. Luikov and Y. Mikhailov: "*Theory of energy and mass transfer*". Prentice Hall U.S.A. (1960).
5) O. Krischer: Chem. Ing. Tech., **34** 154 (1962).
6) E. R. Gilliland, E. R.: Ind. Eng. Chem., **26** 681 (1934).

Nomenclature

A : surface area [m²]
c : local moisture content [kg/kg-dry solid]
c_{f_l} : moisture content at which the internal evaporation appears [kg/kg-dry solid]
c_{f_l}': moisture content at which the liquid moidture transfer ceases [kg/kg-dry solid]
c_m : moisture content at bottom [kg/kg-dry solid]
c_s : moisture content at surface [kg/kg-dry solid]
d_p : diameter of particles [m]
D_v : coefficient of water vapor diffusion in air [m²/hr]
f_l' : local liquid fraction of moisture transfer [−]

h	:	heat transfer coefficient at the surface gas film	[kcal/m²·hr·°C]
k_g	:	mass transfer coefficient at the surface gas film	[m/hr]
k_w	:	interphase evaporation coefficient	[m/hr]
L	:	depth of bed	[m]
p	:	partial pressure of water vapor	[Kg/m²]
p_w	:	saturated vapor pressure of water	[Kg/m²]
R	:	drying rate	[kg/m²·hr]
r	:	latent heat of evaporation of water	[kcal/kg]
R_w	:	gas constant of water vapor	[=47.1 Kg·m/°K·kg]
t	:	temperature	[°C]
w	:	average moisture content	[kg/kg-dry solid]
w_c	:	critical moisture content	[kg/kg-dry solid]
w_p	:	second critical moisture content	[kg/kg-dry solid]
x	:	distance from surface	[m]
δ	:	distance from the surface of the dried-up zone	[m]
ε	:	porosity	[−]
λ	:	effective thermal conductivity of bed	[kcal/m·hr·°C]
μ_1	:	resistance coefficient for vapor diffusion through bed	[−]
ρ'	:	bulk density of dried bed	[kg/m³]
ρ_s	:	density of solid	[kg/m³]
θ	:	time	[hr]

Suffix

a	:	air
c	:	value at w_c
p	:	value at w_p